Surface structures of clean and oxidized Nb(100) by LEED, AES, and STM

B. An,[1] S. Fukuyama,[1] K. Yokogawa,[1,*] and M. Yoshimura[2]
[1]*Institute for Structural and Engineering Materials, National Institute of Advanced Industrial Science and Technology (AIST), AIST-Chugoku, Kure, Hiroshima 737-0197, Japan*
[2]*Toyota Technological Institute, Hisakata, Tempaku, Nagoya 468-8511, Japan*
(Received 6 February 2003; revised manuscript received 2 June 2003; published 25 September 2003)

The surface structures of a Nb(100) single crystal during thermal cleaning in ultrahigh vacuum (UHV) and oxidation in low-pressure oxygen at 300 and 900 K have been studied by combined auger electron spectroscopy, low-energy electron diffraction, and scanning tunneling microscopy. The oxygen-induced (3×1)-O, (4×1)-O, $c(2\times2)$-O, and clean (1×1) structures are sequentially observed on the Nb(100) surface at atomic resolution during thermal cleaning in UHV at temperatures from 1970 to 2500 K. At 300 K, the clean Nb(100) surface is sequentially oxidized into the $c(2\times2)$-O and (1×1)-O structures and the amorphous oxides of NbO and NbO_2 in oxygen. At 900 K, the clean Nb(100) surface is sequentially oxidized into the $c(2\times2)$-O, (4×1)-O, and (3×1)-O structures in oxygen. The $c(2\times2)$-O and (1×1)-O structures result from oxygen chemisorption and the (3×1)-O and (4×1)-O structures result from the epitaxial growth of NbO nanocrystals on Nb(100). Atomic models for these oxygen-induced structures are proposed and the atomic-scale oxidation processes of the Nb(100) surface at 300 and 900 K are discussed.

DOI: 10.1103/PhysRevB.68.115423 PACS number(s): 68.37.Ef, 68.35.Bs, 68.43.Fg, 68.47.Gh

I. INTRODUCTION

Niobium (Nb) has been used for superconducting radio frequency cavities[1] and tunnel barriers in nanoelectronic devices[2] in high technology. However, thin oxide films existing on the Nb surface determine the performance of the application. As is well known, Nb has a very high solubility and binding energy for oxygen, and thus the structure and morphology of the Nb surface in the initial stage of oxidation have been widely studied in the past.[3–20] The structures of the Nb surface during oxidation have been investigated by auger electron spectroscopy (AES),[1,3–8] mirror electron microscopy,[4] secondary ion mass spectroscopy (SIMS),[6,7] ultraviolet photoemission spectroscopy (UPS),[9–11] x-ray photoemission spectroscopy (XPS),[1,10,12,13] and electron energy-loss spectroscopy (EELS).[7,11,14] It has been found that the preparation of a clean Nb surface is very difficult due to its high chemical reactivity.[1,3–7,10,11,14] Clean surfaces could only be obtained by flash heating to temperatures above 2273 K with subsequent rapid cooling in ultrahigh vacuum (UHV).[3–6,14] Exposure of a clean Nb surface to oxygen at room temperature caused the chemisorption of oxygen[6,7,14] and the sequent formation of NbO, NbO_2, and Nb_2O_5 oxides.[6,7,9–11,14] Exposure of a clean Nb surface to oxygen at 900 K caused the chemisorption of oxygen and the formation of only NbO oxide.[6] Nb_2O_5 was reduced into NbO_2 and NbO sequentially during annealing in UHV at temperatures above 598 K due to the dissolution of oxygen into the bulk metal,[8,12,13] and NbO began to evaporate at around 2273 K.[4,14]

The morphology of oxygen-induced structures on Nb(100),[4,5,15,16] Nb(110),[4] and Nb(111) (Ref. 4) surfaces has been investigated by low-energy electron diffraction (LEED). On the Nb(100) surface, a faceted structure,[4,15] a (3×1)-O structure,[15,16] a (4×1)-O structure,[16] a $c(2\times2)$-O structure,[4,15,16] and a clean (1×1) structure[4,5,15,16] were observed during thermal cleaning at temperatures between 1973 and 2673 K in UHV. Exposure of a clean (1×1) surface to oxygen at room temperature resulted in a $c(2\times2)$-O structure[5] and a diffuse (1×1) structure.[4] The (3×1)-O and (4×1)-O structures were assigned to the NbO and Nb_2O oxides on the basis of high-resolution core-level photoemission spectra,[16] and the $c(2\times2)$-O and diffuse (1×1) structures were formed by oxygen chemisorption.[4] However, the geometrical arrangements of the atoms on these oxygen-induced structures could not be clarified.

Recently, the atomic-scale surface structures on Nb(100) (Refs. 17 and 18) and Nb(110) (Refs. 19 and 20) single crystals have been observed by scanning tunneling microscopy (STM). Uehara *et al.*[17] observed pyramided protrusions on Nb(100) after Ar-ion sputtering and heating at 1273 K in UHV, and interpreted the protrusions to be single nanocrystals of NbO grown epitaxially on Nb(100). Li *et al.*[18] observed a ladderlike superstructure on Nb(100) after Ar-ion sputtering and flash heating at 1973 K in UHV. Sürgers *et al.*[19] and Arfaoui *et al.*[20] observed quasiperiodical sticks on Nb(110) after Ar-ion sputtering and annealing in the temperature range of 1200–2200 K in UHV. However, since these observations were carried out independently without starting from a clean (1×1) surface, the evolution of atomic arrangements and their epitaxial relation with the substrate Nb atoms could not be clarified. Consequently, it is important to investigate systematically the atomic structures of Nb surfaces during oxidation starting from the clean surface.

In this study, we have systematically investigated the surface structures formed on a Nb(100) single crystal during thermal cleaning in UHV and oxidation in low-pressure oxygen at 300 and 900 K, by combined AES, LEED, and STM, in order to elucidate the geometrical structures of the oxygen-induced Nb surface and their evolution during cleaning and oxidation. The clean (1×1) structure, the oxygen-induced (3×1)-O, (4×1)-O, $c(2\times2)$-O, and (1×1)-O structures and their conversions during oxidation are ob-

served at atomic resolution, and the atomic models of these structures including the substrate Nb lattice are proposed. It is found that amorphous oxides are formed on the surface during oxidation at 300 K, while epitaxial NbO nanocrystals are formed on the surface during oxidation at 900 K. The atomic-scale oxidation process of the Nb(100) surface is discussed.

II. EXPERIMENT

A Nb(100) single crystal with 99.99% purity and dimensions of $2\times2\times0.3\,\mathrm{mm}^3$ was used as the specimen. The specimen was mounted on a sheet holder made of tantalum of 0.04 mm thickness, which can resistively heat the specimen to 2500 K, and then put into an UHV system equipped with AES, LEED, and STM. The base pressure of the system was below 7×10^{-11} mbar. The main contaminants in the Nb specimen, as detected by AES, were carbon, nitrogen, and oxygen. Thermal cleaning by Ar-ion sputtering at 2.5 keV for 45 min and repeated flash heating in the temperature range of 1970–2500 K for 1–5 min was conducted to clean the specimen surface. The temperature of the specimen was measured using an optical pyrometer set outside the UHV chamber.

Exposure to oxygen was performed by introducing ultrahigh-purity oxygen to the UHV chamber through a variable leak valve, maintaining the partial pressure of oxygen in the range from 7×10^{-9} to 7×10^{-8} mbar for a certain duration. The specimen was held at 300 or 900 K during oxygen exposure.

STM images were observed at room temperature in the UHV chamber. A tungsten rod sharpened by electrochemical etching in KOH solution was used as the STM tip. Further electron bombardment was applied for cleaning the STM tip in UHV before measurement. STM measurements were performed in the constant-current mode at a positive and negative tip bias of 0.02–1.0 V with a tunneling current of 0.2–10 nA. The STM images showed no appreciable bias voltage dependence.

III. RESULTS

A. Cleaning of the Nb(100) surface

Typical LEED patterns and STM images obtained from the Nb(100) surface during thermal cleaning with Ar-ion sputtering and repeated flash heating at elevated temperatures up to 2500 K in UHV are shown in Fig. 1. Two-domain (3×1), two-domain (4×1), $c(2\times2)$, and sharp (1×1) LEED patterns are observed sequentially during thermal cleaning at temperatures from 1970 to 2500 K, as shown in Figs. 1(a), 1(c), 1(f), and 1(h), respectively. AES spectra reveal that only oxygen contamination remains after thermal cleaning above 1970 K. The measured height ratios of the O peak at 510 eV and the Nb peak at 168 eV, I_O/I_{Nb}, for the (3×1), (4×1), $c(2\times2)$, and (1×1) structures are approximately 0.36, 0.26, 0.16, and 0.06, respectively. Thus, the (3×1), (4×1), and $c(2\times2)$ patterns are attributed to oxygen-induced surface structures, and the sharp (1×1) pattern is attributed to the clean (1×1) structure. These changes in superstructure induced by thermal cleaning at elevated temperatures are consistent with the results of previous LEED studies.[4,15,16]

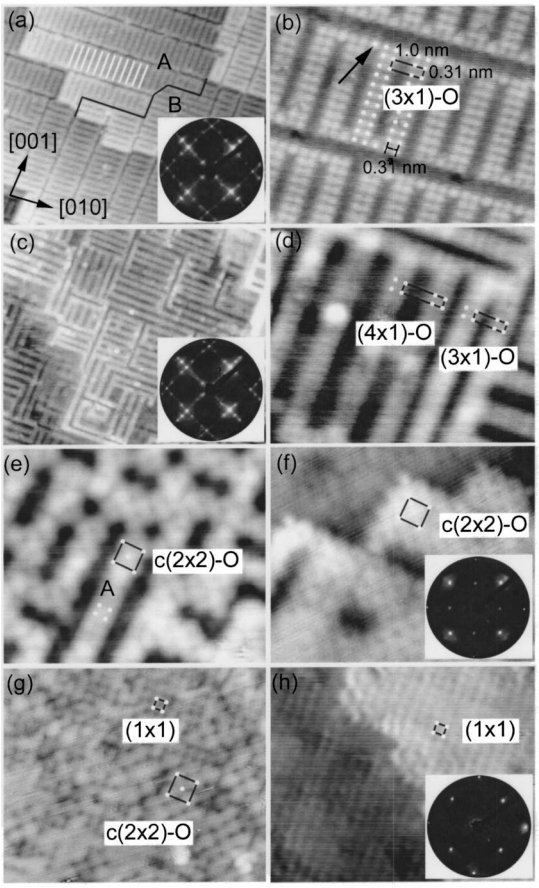

FIG. 1. STM images with LEED patterns of Nb(100) surface obtained during thermal cleaning at elevated temperatures up to 2500 K in UHV. (a) Large-scale image ($40\times33\,\mathrm{nm}^2$) of (3×1)-O structure observed during thermal cleaning at 1970 K. (b) Atomic image ($8.5\times7\,\mathrm{nm}^2$) of the (3×1)-O structure. (c) Large-scale image ($40\times33\,\mathrm{nm}^2$) of (4×1)-O structure observed after flash heating the (3×1)-O structure at 2270 K. (d) Atomic image ($8.5\times7\,\mathrm{nm}^2$) of the (4×1)-O structure. (e) Atomic image ($8.5\times7\,\mathrm{nm}^2$) of $c(2\times2)$-O structures on sticks observed after flash heating the (4×1)-O structure at 2370 K. (f) Atomic image ($8.5\times7\,\mathrm{nm}^2$) of a large domain of $c(2\times2)$-O structure observed after further flash heating. (g) Atomic image ($8.5\times7\,\mathrm{nm}^2$) obtained during transition from the $c(2\times2)$ structure to the clean (1×1) structure upon flash heating at 2500 K. (h) Atomic image ($8.5\times7\,\mathrm{nm}^2$) of the clean (1×1) structure observed after further flash heating at 2500 K.

A large-scale STM image of the (3×1)-O structure observed during thermal cleaning at 1970 K is shown in Fig. 1(a). Flat terraces are observed and two orthogonal domains can be alternately distinguished on each terrace. On the middle terrace, a boundary between two orthogonal domains, as indicated by *A* and *B*, is shown by the black line. Each domain consists of parallel subdomains composed of regular white sticks arranged periodically along the [010] or [001] direction, as shown in the figure. The length of the white sticks depends on the subdomain and is distributed in a range

of 2.7–5.0 nm. Atomically resolved STM images show that the white sticks consist of pairs of small protrusions, as shown in Fig. 1(b). The periodic distance between the white sticks is measured to be approximately 1.0 nm, which is three times the interatomic distance of 0.33 nm along the ⟨100⟩ direction on the Nb(100) plane. Both the periodic distance between the pairs along the stick axis and the distance between the two small protrusions of a pair are around 0.31 nm, which is close to the interatomic distance along the ⟨100⟩ direction on the Nb(100) plane. Thus the subdomain can be described as a (3×1) structure of Nb(100). It is also found that many neighboring sticks are connected at the edge by an additional protrusion, as indicated by an arrow in the image.

A large-scale STM image of the (4×1)-O structure observed after flash heating the (3×1)-O structure at 2270 K is shown in Fig. 1(c). Flat terraces with orthogonal domains consisting of the parallel sticks are also observed on the surface. The length of the sticks is around 2–3 times longer than that on the (3×1)-O structure and the degree of the alignment of the sticks is lower than that on the (3×1)-O structure. Atomically resolved STM images show that the periodic distance between the sticks is four times the interatomic distance along the ⟨100⟩ direction on the Nb(100) plane and the sticks consist of pairs of small protrusions, similar to those on the (3×1)-O structure, as shown in Fig. 1(d), and thus the domain is determined to have a (4×1) structure. The remaining local (3×1)-O structure is partially observed in the image, as shown by the (3×1)-O unit cell.

An atomic STM image of the $c(2\times2)$-O structure observed after flash heating the (4×1)-O structure at 2370 K is shown in Fig. 1(e). The parallel stick features are still observed on the surface. The central part of the stick indicated by A in the image consists of pairs of small protrusions similar to the (4×1)-O structure, while other sticks consist of larger protrusions forming the $c(2\times2)$-O structure. It is found that the protrusions of the $c(2\times2)$-O structure occupy the hollow site between four small protrusions of the (4×1)-O structure. These $c(2\times2)$-O structures on the sticks coalesce into a large domain of $c(2\times2)$-O structure upon further flash heating, as shown in Fig. 1(f).

An atomic STM image observed after flash heating the $c(2\times2)$-O structure at 2500 K is shown in Fig. 1(g). The clean (1×1) structure appears in some regions of the surface and the protrusion of the $c(2\times2)$-O structure is located at the fourfold symmetric hollow site of the clean (1×1) structure. A clean (1×1) structure eventually appears over the entire surface upon further flash heating at 2500 K, as shown in Fig. 1(h). Such atomic STM images of clean (1×1) structures could only be obtained with a very sharp tip at a low bias voltage of 20–50 mV and a high tunnel current of 5–10 nA. The atomic corrugation of the clean (1×1) structure is measured to be approximately 13 pm. As far as we know, this is the first report of an atomic STM image of the clean Nb surface.

B. Oxidation of a clean Nb(100) surface at 300 and 900 K

Typical STM images together with LEED patterns obtained after exposing a clean Nb(100) surface to 0.2–64 L of oxygen at 300 K are shown in Fig. 2. The clean (1×1) structure is converted into the $c(2\times2)$-O structure upon exposure to a very small amount of oxygen (~0.2 L), as shown in Fig. 2(a). The corresponding LEED pattern shows a $c(2\times2)$ structure, which is in agreement with the STM image, as shown in the inset of Fig. 2(a). The I_O/I_{Nb} value of the $c(2\times2)$-O structure is measured to be approximately 0.16. The $c(2\times2)$-O structure is further converted into a (1×1)-O structure by increasing the amount of oxygen exposure to 0.4 L, as shown in Fig. 2(b). Both the $c(2\times2)$-O and (1×1)-O structures are observed in the image. The (1×1)-O structure covers the entire surface after increasing oxygen exposure to 0.6 L, as shown in Fig. 2(c). It is found that the (1×1)-O structure consists of small (1×1)-O patches divided by short bright orthogonal lines, as indicated by the white lines. The atomic corrugation of the (1×1)-O structure is measured to be approximately 30 pm, which is 2.3 times that of the clean (1×1) structure. The corresponding LEED pattern shows diffuse (1×1) spots with satellite spots, as shown in the inset of Fig. 2(c). The I_O/I_{Nb} value of the (1×1)-O structure is measured to be approximately 0.23. When the oxygen exposure is increased to around 1.5 L, the (1×1)-O structure becomes disordered and a bright clusterlike structure appears on the surface, as shown in Fig. 2(d), where the bright clusterlike structure is indicated by an arrow. After increasing oxygen exposure to around 3.0 L, the clusterlike structure covers the entire surface, as shown in Fig. 2(e). The diffraction spots of the surface became weaker

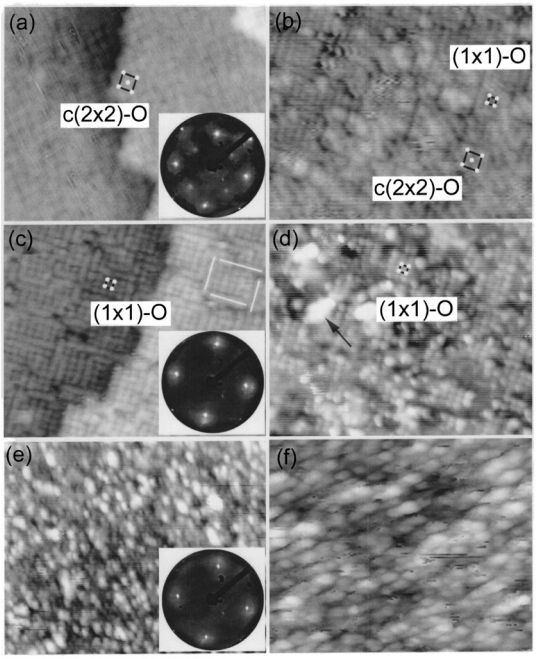

FIG. 2. STM images (11×9 nm^2) with LEED patterns obtained after exposing a clean Nb(100) surface to 0.2–64 L of oxygen at 300 K. (a) $c(2\times2)$-O structure after exposure to 0.2 L. (b) $c(2\times2)$-O and (1×1)-O structures after exposure to 0.4 L. (c) (1×1)-O structure after exposure to 0.6 L. (d) (1×1)-O structure with small clusters after exposure to 1.5 L. (e) Small clusters on entire surface after exposure to 3 L. (f) Larger clusters after exposure to 64 L.

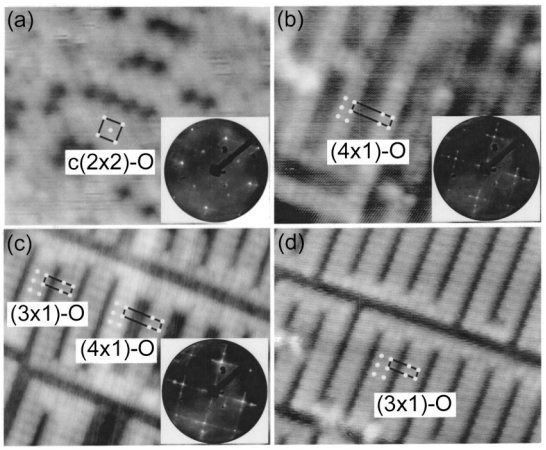

FIG. 3. STM images (8.5×7 nm^2) with LEED patterns obtained after exposing a clean Nb(100) surface to 0.2–300 L of oxygen at 900 K. (a) $c(2\times2)$-O structure after exposure to 0.2 L. (b) (4×1)-O structure after exposure to 0.8 L. (c) (3×1)-O structure with partial (4×1)-O structure after exposure to 3 L. (d) (3×1)-O structure after exposure to 300 L.

by cluster formation, as shown in the inset of Fig. 2(e). Further exposure of oxygen leads to the growth of clusterlike structures and complete disappearance of the diffraction spots. A STM image obtained after exposure to 64 L of oxygen is shown in Fig. 2(f). The clusterlike structure is larger than that in Fig. 2(e). No atomic structure or diffraction spots are observed for this surface. It is also noted that STM observation of this surface requires a high bias voltage of 1.0 V. The I_O/I_{Nb} value changes from 0.38 to 0.54 on increasing the oxygen exposure from 3 to 64 L. This clusterlike structure is changed into the (3×1)-O structure upon heating above 870 K in UHV, and the (3×1)-O structure is subsequently converted into the (4×1)-O, $c(2\times2)$-O, and clean (1×1) structures with further heating at elevated temperatures up to 2500 K in UHV, as in the cleaning process in Fig. 1.

Typical STM images together with LEED patterns obtained after exposing a clean Nb(100) surface to 0.2–300 L of oxygen at 900 K are shown in Fig. 3. The clean (1×1) structure is converted into the $c(2\times2)$-O structure upon exposure to 0.2 L of oxygen, as shown in Fig. 3(a). The corresponding LEED pattern shows a $c(2\times2)$ structure, which is in agreement with the STM image, as shown in the inset of Fig. 3(a). The I_O/I_{Nb} value of the $c(2\times2)$-O structure is measured to be approximately 0.18. The $c(2\times2)$-O structure is further converted into the (4×1)-O structure by increasing oxygen exposure to above 0.6 L. A STM image of the (4×1)-O structure obtained after exposure to 0.8 L of oxygen is shown in Fig. 3(b). The corresponding LEED pattern shows the (4×1) structure, which is in agreement with the STM image, as shown in the inset of Fig. 3(b). The I_O/I_{Nb} value of the (4×1)-O structure is measured to be approximately 0.27. When oxygen exposure is increased to around 1.5 L, the (4×1)-O structure is converted into the (3×1)-O structure. A STM image of the (3×1)-O structure obtained after exposure to 3 L of oxygen is shown in Fig. 3(c). The (4×1)-O structure is partially observed in the image, as shown by the (4×1)-O unit cell. The corresponding LEED pattern shows the (3×1) structure, which is in agreement with the STM image, as shown in the inset of Fig. 3(c). The I_O/I_{Nb} value of the (3×1)-O structure is measured to be approximately 0.38. The (3×1)-O structure remains unchanged with exposure to up to at least 300 L of oxygen, as shown in Fig. 3(d). The $c(2\times2)$-O, (4×1)-O, and (3×1)-O structures observed during oxidation at 900 K coincide with those observed during the cleaning process. These results reveal that the oxidation process of the Nb(100) surface at 900 K is different from that at 300 K.

IV. DISCUSSION

On the basis of the above results, we propose possible atomic models for the oxygen-induced surface structures of Nb(100), (3×1)-O, (4×1)-O, $c(2\times2)$-O, and (1×1)-O structures, as shown in Fig. 4, and discuss the atomic-scale oxidation process of the Nb(100) surface.

A. (3×1)-O structural model

We observed the (3×1)-O structure of Nb(100) after three different treatments: thermal cleaning of the Nb(100) single crystal at 1970 K in UHV [Figs. 1(a) and 1(b)]; exposing the clean Nb(100) surface to 64 L of oxygen at 300 K and then heating in UHV at 870 K; and exposing the clean Nb(100) surface to more than 1.5 L of oxygen at 900 K [Figs. 3(c) and 3(d)]. A similar (3×1)-O structure of Nb(100) was observed previously by LEED in the initial stages of similar thermal cleaning[15,16] and identified as the NbO component by high-resolution core-level photoemission.[16] It was also reported that the exposure of the polycrystalline Nb surface to oxygen at 900 K resulted in the formation of NbO oxide only.[6] The NbO crystal has a NaCl structure and presents metallic properties.[17,19,20] In the present STM images, the (3×1)-O structure consists of the periodically parallel white sticks along the [010] or [001] direction of the Nb(100) surface with a periodic distance of around 1.0 nm, which is three times the interatomic distance of 0.33 nm along the $\langle100\rangle$ direction on the Nb(100) plane. The white stick is composed of pairs of small protrusions, where both the periodic distance between the pairs along the stick axis and the distance between two small protrusions of a pair are around 0.31 nm [Fig. 1(b)], which is close not only to the interatomic distance along the $\langle100\rangle$ direction on the Nb(100) plane but also to the interatomic distance of 0.298 nm along the $\langle110\rangle$ direction on the NbO(100) surface. At low bias voltages, since the transition metal atoms usually appear as bright protrusions and the oxygen atoms as dark depressions due to the lower density of states (DOS) near the Fermi energy above the oxygen position after oxygen adsorption by STM (Refs. 21–23) especially and, in particular, the Nb atoms appear as bright protrusions on the oxygen-induced superstructure of Nb(110),[19] it is considered that the protrusions in STM images observed in this study can also be assigned to Nb atoms. Thus the (3×1)-O structure is explained in terms of the epitaxial growth of a NbO(100) layer on Nb(100) with in-plane orientation,

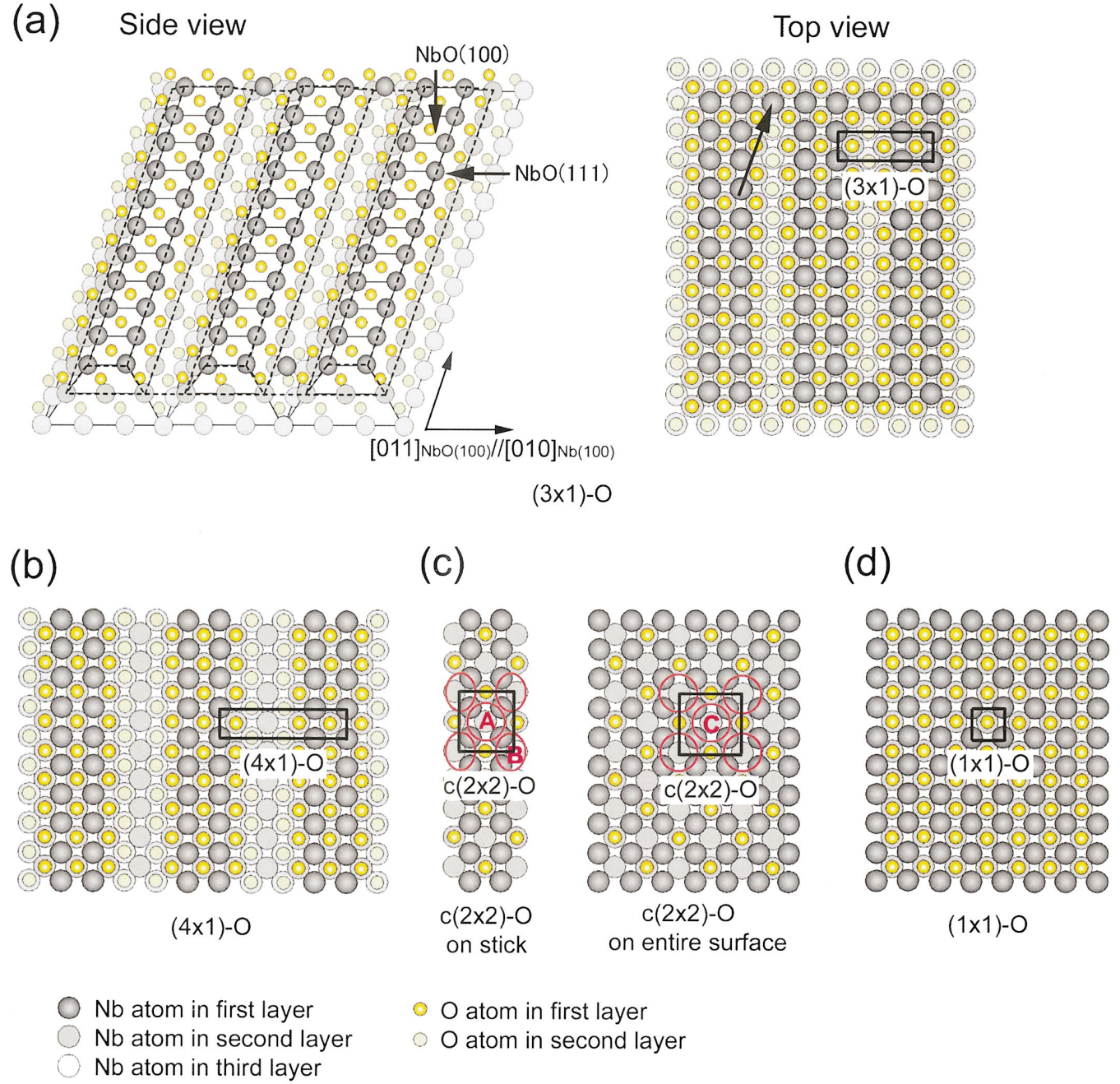

FIG. 4. (Color) Atomic models of oxygen-induced surface structures of Nb(100). (a) Side and top views of (3×1)-O structure. (b) Top view of (4×1)-O structure. (c) Top view of $c(2\times2)$-O structure. (d) Top view of (1×1)-O structure.

NbO[011]//Nb[010] and NbO[$0\bar{1}1$]//Nb[001]. Lo *et al.*[16] showed that the Nb 3*d* core-level photoemission spectra on the (3×1)-O structure contained both the oxide-related peaks and pure niobium-related peaks. Considering the very short escape length for 50–55 eV photoelectrons,[20,24] we estimate that 1–3 layers of oxide exist on the surface. Side and top views of the (3×1)-O structural model are shown in Fig. 4(a), in which two-layer oxides are formed. The large black spheres, gray circles, and white circles indicate Nb atoms in the first, second, and third layers, respectively. The small yellow spheres and circles indicate oxygen atoms in the first and second layers, respectively. In the top view of the model, every third Nb atom row is missing from the first layer of NbO(100) along the NbO[011]//Nb[010] direction and every twelfth Nb atom row is missing along the NbO[$0\bar{1}1$]//Nb[001] direction. The remaining Nb atoms in the first layer of NbO(100) appear in the STM images as parallel sticks consisting of pairs of small protrusions. An additional Nb atom, indicated by an arrow in the figure, corresponds to the additional protrusion indicated by an arrow in Fig. 1(b). In the side view of the model, the sticks are composed of NbO nanocrystals and are indicated by the dotted lines. The top face of a nanocrystal is the NbO(100) face and the side face is the NbO(111) face, as indicated in the

model. Thus, the (3×1)-O structure can also be described as a side-to-side arrangement of epitaxial NbO nanocrystals on Nb(100). Arfaoui *et al.*[20] also observed short parallel sticks on the Nb(110) surface by STM after Ar-ion sputtering and annealing in the temperature range of 1200–2200 K, and identified the sticks to be nanosize NbO crystals formed by the misfit between NbO(111) and Nb(110). Thus, it is considered that the (3×1)-O structure of Nb(100) observed in this study is caused by the misfit between NbO(100) and Nb(100). The misfit value of NbO(100)/Nb(100) along their common direction, NbO$\langle011\rangle$//Nb$\langle010\rangle$, is approximately 10%. We consider that this misfit leads to the loss of each third Nb atom row with NbO[011] or NbO[$\underline{0}$11] orientation and each twelfth Nb atom row with NbO[011] or NbO[011] orientation.

B. (4×1)-O structural model

We observed the (4×1)-O structure after flash heating the (3×1)-O structure at 2270 K in UHV [Figs. 1(c) and 1(d)] and after exposing the clean Nb(100) surface to 0.4–1.5 L of oxygen at 900 K [Fig. 3(b)]. It has been reported that NbO begins to evaporate from the surface at around 2273 K.[4,14] The present STM images show that the (4×1)-O structure also consists of the parallel sticks composed of pairs of small protrusions, similar to those observed on the (3×1)-O structure. However, the periodic distance between the sticks is four times the interatomic distance along the $\langle100\rangle$ direction on the Nb(100) plane and the length of the sticks is around 2–3 times longer than that on the (3×1)-O structure. Thus, the (4×1)-O structure can be explained as resulting from the removal of NbO oxide from the (3×1)-O structure due to the evaporation of NbO from the surface. A top view of the (4×1)-O structural model is shown in Fig. 4(b). The periodic interval of the NbO nanocrystals becomes larger, from three to four times the interatomic distance along the $\langle100\rangle$ direction on the Nb(100) plane due to the additional removal of NbO oxide from the (3×1) structure. As a result, the strains induced by NbO/Nb misfit are more relaxed and longer NbO nanocrystals can be formed.

C. $c(2\times2)$-O structural model

We observed the $c(2\times2)$-O structure after flash heating the (4×1)-O structure at 2370 K in UHV [Figs. 1(e) and 1(f)] and after exposing the clean Nb(100) surface to 0.2–0.4 L of oxygen at 300 and 900 K [Figs. 2(a) and 3(a)]. The $c(2\times2)$-O structure was observed previously by LEED (Refs. 4, 5, 15, 16) and interpreted as resulting from oxygen chemisorption on the Nb(100) surface.[4] The present STM images show that the $c(2\times2)$-O structures form on the sticks of the (4×1)-O structure [Fig. 1(e)] and coalesce into a large domain of the $c(2\times2)$-O structure upon further flash heating in UHV [Fig. 1(f)]. The protrusions of the $c(2\times2)$-O structure are larger than those of Nb atoms on the (3×1)-O and (4×1)-O structure and are located at the hollow position between four Nb atoms. Thus, the $c(2\times2)$-O structure is interpreted as resulting from oxygen chemisorption at the hollow position between four Nb atoms of the Nb(100) surface with $c(2\times2)$ periodicity. A top view of the $c(2\times2)$-O structural model is shown in Fig. 4(c). The $c(2\times2)$-O structure on a stick is shown in the left part of the figure, in which the oxygen atoms remaining after oxygen desorption from the (4×1)-O structure form a $c(2\times2)$ structure on the stick. Four Nb atoms without oxygen at the center appear in the STM image as a large protrusion on the top of the stick, as indicated by circle A. Three Nb atoms, including two Nb atoms of the first layer and one Nb atom of the second layer without oxygen at the top, appear in the STM image as a large protrusion on the side of the stick, as indicated by an oval B. A large domain of the $c(2\times2)$-O structure is shown in the right part of the figure, in which the oxygen atoms form a $c(2\times2)$ structure over the entire surface. Four Nb atoms without oxygen at the center appear in the STM image as a large protrusion, as indicated by circle C. Koller *et al.*[23] observed a $c(2\times2)$-O structure on a V(100) surface by STM and simulated the STM images by density functional theory calculation. Their experiments and simulation also revealed that the fourfold symmetric hollow sites occupied by the oxygen atoms appear as dark depressions, while the unoccupied hollow sites remain bright protrusions, similar to the present study.

D. (1×1)-O structural model

We observed the (1×1)-O structure after exposing the clean (1×1) structure to 0.4–1.5 L of oxygen at 300 K [Figs. 2(b) and 2(c)]. The LEED pattern shows diffuse (1×1) spots with satellite spots [inset of Fig. 2(c)]. A similar diffuse (1×1) structure was observed previously by LEED after exposure of clean Nb(100) to oxygen at room temperature and considered to be caused by oxygen chemisorption.[4] Rieder[7] concluded, from the results of LEED, AES, SIMS, and ELS studies, that the oxygen was chemisorbed on the Nb(110) surface by exposure to less than 1.7 L of oxygen at room temperature. The (1×1)-O structure consists of (1×1)-O patches divided by the short lines in the present STM images [Fig. 2(c)] and the atomic corrugation of the (1×1)-O structure is 2.3 times that of the clean (1×1) structure. Thus, we consider that the (1×1)-O structure is due to monolayer oxygen chemisorption on the Nb(100) surface. A top view of the (1×1)-O structural model is shown in Fig. 4(d), in which the oxygen atoms occupy all the hollow positions between four Nb atoms. The high degree of atomic corrugation of the (1×1)-O structure is considered to be due to the modulation of the electronic states of the Nb atom as a result of oxygen adsorption. Wolter *et al.*[25] frequently observed similar line boundaries on heteroepitaxial films and concluded that the line boundaries were formed due to the relaxation of surface distortion. Thus, the short line boundaries, which divide the (1×1)-O structure into small patches, are considered to form due to the relaxation of surface distortion induced by oxygen adsorption.

E. Oxidation process of Nb(100) surface

On the basis of the above STM observations and structural models, the oxidation process of Nb(100) at 300 K is

interpreted as follows. (i) Exposure to 0.2–0.4 L of oxygen results in the $c(2\times2)$-O structure [Fig. 2(a)]. Oxygen is dissociatively chemisorbed with $c(2\times2)$ periodicity at the hollow position between four Nb atoms on the Nb(100) surface in this stage [Fig. 4(c)]. (ii) Increasing oxygen exposure from 0.4 to 1.5 L results in a conversion from $c(2\times2)$-O to (1×1)-O [Figs. 2(b) and 2(c)]. This reveals that the oxygen atoms occupy all the hollow positions between four Nb atoms on the Nb(100) surface [Fig. 4(d)]. (iii) Further increase of the amount of oxygen exposure to above 1.5 L causes the formation of the clusterlike structure [Figs. 2(d) and 2(e)]. The clusterlike structure grows with increasing oxygen exposure up to 64 L and its STM images are obtained at higher bias voltages up to 1.0 V [Fig. 2(f)]. Rieder[7] reported that the NbO and NbO_2 oxides formed on the Nb(110) surface after exposure to 1.7–5.5 L of oxygen at room temperature and further exposure to 5.5–300 L of oxygen resulted in the formation of Nb_2O_5 oxide. Franchy *et al.*[14] suggested that NbO and NbO_2 clusters were first formed on the Nb(110) surface on exposure to oxygen at 300 K and the Nb_2O_5 islands were formed upon further exposure. It was also reported that the NbO oxide presents metallic properties, while the oxygen-rich oxides, such as NbO_2 and Nb_2O_5, have semiconductive and insulative properties, respectively.[17,20] Thus, the clusterlike structure formed in this stage is considered to be composed of amorphous NbO and NbO_2 oxides. These clusterlike amorphous structures are changed into the (3×1)-O structure upon heating in UHV at temperatures above 870 K. This reveals that the amorphous NbO and NbO_2 oxides are crystallized into epitaxial NbO nanocrystals via the dissolution of oxygen into the bulk metal during heating in UHV.

The oxidation process of Nb(100) at 900 K is found to be different from that at 300 K, and is interpreted as follows. (i) Exposure to 0.2–0.6 L of oxygen also results in the $c(2\times2)$-O structure [Fig. 3(a)]. It reveals that the behavior of oxygen in the first stage of oxygen exposure at 900 K is similar to that at 300 K. (ii) Increase of the oxygen exposure from 0.6 to 1.5 L results in a conversion from $c(2\times2)$-O to (4×1)-O [Fig. 3(b)]. This reveals that the (4×1)-O structure is more thermodynamically stable than the (1×1)-O structure. (iii) Further increase of the oxygen exposure to above 1.5 L results in the (3×1)-O structure [Fig. 3(c)]. The (3×1)-O structure is stable at least up to 300 L. This is consistent with the SIMS result that only the NbO oxide was produced on the Nb surface after oxidation in low-pressure oxygen at 900 K.[6] These results reveal that epitaxial NbO oxide grows on the surface during oxidation at elevated temperatures due to the diffusion of oxygen into the bulk metal, while amorphous oxides are formed on the surface during oxidation at room temperature due to the difficulty of oxygen diffusion.

V. CONCLUSION

We have studied the surface structures formed on a Nb(100) single crystal during thermal cleaning in UHV and oxidation in low-pressure oxygen at 300 and 900 K, by combined AES, LEED, and STM. The oxygen-induced (3×1)-O, (4×1)-O, $c(2\times2)$-O, and clean (1×1) structures are sequentially observed on the Nb(100) surface at atomic resolution during thermal cleaning in UHV at temperatures from 1970 to 2500 K. The (3×1)-O structure consists of the periodically parallel sticks composed of the pairs of Nb atoms, and is explained in terms of the epitaxial growth of NbO(100) nanocrystals with a side-to-side arrangement on Nb(100) due to the misfit of NbO(100)/Nb(100). For each stick of NbO(100) nanocrystal, one $\langle011\rangle$ direction is parallel to one $\langle010\rangle$ direction of the Nb(100) plane. The (4×1)-O structure also consists of the periodically parallel sticks of NbO(100) nanocrystals similar to those of (3×1)-O structure. However, the periodic interval of the sticks becomes larger, from three to four times the interatomic distance on the Nb(100) plane, and the length of the sticks becomes 2–3 times longer than that on the (3×1)-O structure, due to the additional removal of NbO oxide from the (3×1)-O structure and the relaxation of the strains induced by the misfit of NbO/Nb. The $c(2\times2)$-O structures form on the sticks of the (4×1)-O structure and coalesce into a large domain. The protrusion of the $c(2\times2)$-O structure is located at the hollow position between four Nb atoms and is larger than those of Nb atoms on the (4×1)-O and clean (1×1) structures. Thus, the $c(2\times2)$-O structure is interpreted as resulting from the oxygen chemisorption at the hollow positions between four Nb atoms of the Nb(100) surface with $c(2\times2)$ periodicity.

In the oxidation at 300 K, the clean (1×1) structure is sequentially converted into the $c(2\times2)$-O and (1×1)-O structures by exposure to 0.2–1.5 L of oxygen and into the clusterlike structure by exposure to 1.5–64 L of oxygen. The (1×1)-O structure consists of small (1×1)-O patches, resulting from the relaxation of surface distortion induced by oxygen adsorption. The clusterlike structure results from the growth of amorphous oxides of NbO and NbO_2, which are crystallized into the (3×1)-O structure via the dissolution of oxygen into the bulk metal during heating at above 870 K in UHV. In the oxidation at 900 K, on the other hand, the clean (1×1) structure is sequentially converted into the $c(2\times2)$-O and (4×1)-O structures by exposure to 0.2–1.5 L of oxygen and into the (3×1)-O structure by exposure to 1.5–300 L of oxygen. These indicate that epitaxial NbO oxide grows on the surface during oxidation at elevated temperatures due to the diffusion of oxygen into the bulk metal, while amorphous oxides form on the surface during oxidation at room temperature due to the difficulty of oxygen diffusion.

Based on the above systematic real space observations, atomic models for the oxygen-induced (3×1)-O, (4×1)-O, $c(2\times2)$-O, and (1×1)-O structures on Nb(100) are proposed and the atomic-scale oxidation processes of the Nb(100) surface at 300 and 900 K are discussed. Finally, theoretical simulations about these atomic models would be necessary to provide more convincing information on this technologically important system.

*Email address: yokogawa.kiyoshi@aist.go.jp

[1] M. Grundner and J. Halbritter, J. Appl. Phys. **51**, 397 (1980).
[2] J. Shirakashi, K. Matsumoto, N. Miura, and M. Konagai, J. Appl. Phys. **83**, 5567 (1998).
[3] H. H. Farrell, H. S. Isaacs, and M. Strongin, Surf. Sci. **38**, 31 (1973).
[4] R. Pantel, M. Bujor, and J. Bardolle, Surf. Sci. **62**, 589 (1977).
[5] S. Usami, N. Tominaga, and T. Nakajima, Vacuum **27**, 11 (1977).
[6] P. H. Dawson and W.-C. Tam, Surf. Sci. **81**, 464 (1979).
[7] K. H. Rieder, Appl. Surf. Sci. **4**, 183 (1980).
[8] H. Oechsner, J. Giber, H. J. Füßer, and A. Darlinski, Thin Solid Films **124**, 199 (1985).
[9] I. Lindau and W. E. Spicer, J. Appl. Phys. **45**, 3720 (1974).
[10] Z. P. Hu, Y. P. Li, M. R. Ji, and J. X. Wu, Solid State Commun. **71**, 849 (1989).
[11] Y. Wang, X. Wei, Z. Tian, Y. Cao, R. Zhai, T. Ushikubo, K. Sato, and S. Zhuang, Surf. Sci. **372**, L285 (1997).
[12] B. R. King, H. C. Patel, D. A. Gulino, and B. J. Tatarchuk, Thin Solid Films **192**, 351 (1990).
[13] A. Daccà, G. Gemme, L. Mattera, and R. Parodi, Appl. Surf. Sci. **126**, 219 (1998).
[14] R. Franchy, T. U. Bartke, and P. Gassmann, Surf. Sci. **366**, 60 (1996).
[15] H. H. Farrell and M. Strongin, Surf. Sci. **38**, 18 (1973).
[16] W. S. Lo, H. H. Chen, T. S. Chien, C. C. Tsan, and B. S. Fang, Surf. Rev. Lett. **4**, 651 (1997).
[17] Y. Uehara, T. Fujita, M. Iwami, and S. Ushioda, Surf. Sci. **472**, 59 (2001).
[18] Y. Li, B. An, X. Xu, S. Fukuyama, K. Yokogawa, and M. Yoshimura, J. Appl. Phys. **89**, 4772 (2001).
[19] C. Sürgers, M. Schöck, and H. Löhneysen, Surf. Sci. **471**, 209 (2001).
[20] I. Arfaoui, J. Cousty, and H. Safa, Phys. Rev. B **65**, 115413 (2002).
[21] J. Wintterlin, J. Trost, S. Renisch, R. Schuster, T. Zambelli, and G. Ertl, Surf. Sci. **394**, 159 (1997).
[22] M. Schmid, G. Leonardelli, M. Sporn, E. Platzgummer, W. Hebenstreit, M. Pinczolits, and P. Varga, Phys. Rev. Lett. **82**, 355 (1999).
[23] R. Koller, W. Bergermayer, G. Kresse, E. L. D. Hebenstreit, C. Konvicka, M. Schmid, R. Podloucky, and P. Varga, Surf. Sci. **480**, 11 (2001).
[24] C. R. Brundle, Surf. Sci. **48**, 99 (1975).
[25] H. Wolter, K. Meinel, Ch. Ammer, K. Wandelt, and H. Neddermeyer, Phys. Rev. B **56**, 15 459 (1997).